This is an *Accepted Manuscript*, which has been through the Royal Society of Chemistry peer review process and has been accepted for publication.

Accepted Manuscripts are published online shortly after acceptance, before technical editing, formatting and proof reading. Using this free service, authors can make their results available to the community, in citable form, before we publish the edited article. We will replace this *Accepted Manuscript* with the edited and formatted *Advance Article* as soon as it is available.

You can find more information about *Accepted Manuscripts* in the **Information for Authors**.

Journal Name

ARTICLE

High Electrical Conductivity of Double-Walled Carbon Nanotube Fibers by Hydrogen Peroxide Treatments

A. Morelos-Gómez,*[ab] M. Fujishige,[a] S. Magdalena Vega-Díaz,[c] I. Ito,[ab] T. Fukuyo,[d] R. Cruz-Silva,[bc] F. Tristán-López,[c] K. Fujisawa,[e] T. Fujimori,[c] R. Futamura,[c] K. Kaneko,[c] K. Takeuchi,*[ab] T. Hayashi,[e] Y. A. Kim,[f] M. Terrones,[cg] M. Endo*[ab] and M. S. Dresselhaus[h]

Double-walled carbon nanotube (DWNT) fibers are of great interest due to their electrical properties and light weight, making them attractive for industrial applications including their potential use in power transmission lines. We present here a detailed study of the mechanism by which hydrogen peroxide (H_2O_2) treatment improves the electrical transport of DWNT fibers. These fibers were immersed and sonicated in H_2O_2 for several hours. Experimental results suggest that residual H_2O2 could be intercalated within intertube channels inside the bundles of DWNTs, and the oxidation treatment could also result in the removal of small diameter carbon nanotubes (CNTs). In addition, an increase in the fiber density resulted in a decrease of the electrical resistivity. The H_2O_2 treatment of the DWNT fibers resulted in a metallic-like temperature dependent resistivity behavior with a transition to a semiconducting-like behavior below 30 K. We compared the effects of H_2O_2 with other well-known solvents and additives commonly used to reduce the carbon nanotube fiber electrical resistivity and found that the electrical conductivity values observed in our study are as good as those obtained with thionyl chloride and iodine additives. The H_2O_2 method was also used to treat other forms of carbon, where only the multi-walled carbon nanotubes doped with nitrogen exhibited a decrease in electrical resistivity. The fabrication method presented here is simple, efficient and low cost, thus making it an ideal process to be applied in the fabrication of electrically conducting carbon nanotube fibers.

Introduction

Since the development of the well-established production process for nanoscale carbon fibers based on the catalytic chemical vapor deposition (CCVD) method,[1,2] and the subsequent recognition that these fibers are members of the fullerene family[3,4] now called carbon nanotubes (CNTs), the electrical and mechanical properties of single-, double- and multi-walled carbon nanotubes (SWNTs, DWNTs and MWNTs)

have been widely and actively studied.[5-7] One of the outstanding properties of these materials is their high electrical conductivity. For example, SWNT-based ropes may exhibit electrical resistivity as low as 10^{-4} Ω·cm.[8-10] In particular, pristine DWNTs could exhibit electrical resistivity values ranging between 10^{-2} Ω·cm and 10^{-4} Ω·cm,[11,12] with lower electrical resistivities than SWNTs.[13] Unfortunately, many synthetic methods yield a mixture of semiconducting and metallic CNTs, and in addition, catalyst nanoparticles and amorphous carbon could be present within the samples. The different types of nanotubes and impurities from the synthesis will affect the electrical properties, resulting in increased resistivity values. Therefore, further research needs to be conducted in order to address these critical issues.

Doping and intercalation processes have been widely used to decrease the electrical resistivity of CNTs, in a similar way as is done in graphite intercalation compounds.[14] One approach consists of exohedral doping with potassium, bromine or iodine. CNTs doped with potassium or bromine could exhibit resistivity values ranging between 10^{-3} and 10^{-4} Ω·cm.[15,16] In particular, DWNT ropes doped with iodine could yield low electrical resistivities in the order of 10^{-5} Ω·cm.[11] Other chemical treatments with molecules, such as HNO_3, H_2SO_3, H_2SO_4, $NH_4S_2O_8$, $SOCl_2$, yielded electrical resistivity values ranging between 10^{-3} and 10^{-5} Ω·cm.[13,17-22] In-plane doping, by the substitution of carbon atoms with nitrogen atoms could also decrease the electrical resistivity of CNTs to values of ca.

a. Institute of Carbon Science and Technology, Shinshu University, 4-17-1 Wakasato, Nagano-city 380-8553, Japan.
b. Global Aqua Innovation Center, Shinshu University, 4-17-1 Wakasato, Nagano 380-8553, Japan. endo@endomoribu.shinshu-u.ac.jp, takeuchi@endomoribu.shinshu-u.ac.jp, amorelos@shinshu.ac.jp
c. Research Center for Exotic Nanocarbons (JST), Shinshu University, 4-17-1 Wakasato, Nagano-city 380-8553, Japan.
d. MEFS Co., Ltd., Nagano-city 380-0921, Japan.
e. Faculty of Engineering, Shinshu University, 4-17-1 Wakasato, Nagano-city 380-8553, Japan.
f. School of Polymer Science and Engineering, Chonnam National University, 77 Yongbong-ro, Buk-gu, Gwangju, 500-757, Korea.
g. Department of Physics, Department of Chemistry, Department of Material Science and Engineering and Center for 2-Dimensional and Layered Materials, The Pennsylvania State University, University Park, Pennsylvania 16802, USA.
h. Department of Electrical Engineering and Computer Science and Department of Physics, Massachusetts Institute of Technology, Cambridge, Massachusetts 02139-4307, USA.
† The current address of AMG, RCS and II is Global Aqua Innovation Center
Electronic Supplementary Information (ESI) available: [details of any supplementary information available should be included here]. See DOI: 10.1039/x0xx00000x

2.4×10^{-3} $\Omega \cdot$cm.[23] Unfortunately, the majority of the molecules used in these procedures are highly toxic, and could be hazardous and risky for the development of large-scale applications. In addition, various intercalation methods require the use of controlled atmospheres because of their air sensitivity and instability at elevated temperatures.

H_2O_2 is well known to react mildly with graphitic carbon and to purify carbon nanotube samples,[11,12] and could decrease the electrical resistivity of DWNTs to 10^{-3} $\Omega \cdot$cm.[12] Wei et al. attributed the decrease of the electrical resistivity due to the surface purification of their samples; however, they did not consider other possible mechanisms.[12] Zhao et al. also used H_2O_2 for the purification of their DWNT fiber.[11] However, they thermally oxidize their sample before the H_2O_2 treatment. Afterwards, they continue to treat their sample with HCl. Unfortunately, they did not study the intermediate steps (thermal oxidation, hydrogen peroxide treatment and HCl treatment) to monitor how the electrical resistivity changes during each step and how each intermediate step contributes to understanding the role of the overall H_2O_2 treatment.

H_2O_2 treatments have been reported to remove small diameter semiconducting SWNTs by selective oxidation, when the suspensions were heated between 50 ^{o}C and 90 ^{o}C, and in a particular case aided by laser irradiation.[24,25] Here, we report a detailed study aimed at elucidating the mechanism whereby the electrical resistivity of DWNT ropes sonicated with H_2O_2 is reduced. Our results indicate that the decrease in resistivity is caused by the removal of small diameter semiconducting CNTs and by an increase in the fiber density that could further enhance the electrical transport within DWNTs. We found that the H_2O_2 treatment could reduce the electrical resistivity from the pristine value of 4.19×10^{-3} $\Omega \cdot$cm to 2.77×10^{-4} $\Omega \cdot$cm. This method is low cost, simple, and effective to reach low electrical resistivity values that are commercially attractive, and more importantly, could be easily scaled up. In addition, this method is safer than others which rely on more aggressive solvents and additives, such as thionyl chloride, iodine, nitric acid, sulfuric acid, among others.

Experimental

Double walled nanotubes (DWNTs) were synthesized by chemical vapor deposition (CVD) with a floating catalyst process.[1,2] The carbon feedstock contained decahydronaphthalene, thiophene and ferrocene, with a ratio of 100:1.5:1.5. The CVD reaction was carried out in the presence of hydrogen at a temperature of 1300 ^{o}C. The obtained material (Figure 1) was in the form of a DWNT net form.

The net was twisted by hand and soaked in acetone (Figure 1c,d and e), to allow certain shrinkage during the acetone evaporation; this sample is labeled as a DWNT. The DWNT was then immersed in hydrogen peroxide (34.5%) and sonicated in an ultrasonic bath for a time between 20 and 30 hours. After sonication, the sample was dried at 90 ^{o}C and soaked in acetone for further twisting; this sample is labeled as DWNT-H_2O_2 (Figure 1f,g, and h). For other treatments, the fibers were also twisted in acetone after the treatment. For chemical doping, the DWNT fiber was sonicated in $SOCl_2$ (95%) and in NH_4OH (28%) for 3 hours, and then dried; shorter times were

used due to the complete decomposition of the fiber morphology after prolonged sonication. The silver nanoparticles were synthesized following the method reported by Coskun et al.[26] Here 10 ml of 0.45 M ethylene glycol solution of poly(vinylpyrrolidone) (MW=55000), was mixed and then 7 mg of NaCl was added at room temperature. Subsequently, the solution was heated to 170 ^{o}C and 0.21 M of $AgNO_3$ in ethylene glycol was added manually dropwise into the first solution accompanied by magnetic stirring at ca. 1000 rpm. The solution was left at 170 ^{o}C for 30 minutes and then left to cool to room temperature. Finally, the solution was centrifuged at 4000 rpm and the supernatant was collected. Later the fibers were soaked in the supernatant solution containing the silver particles, then dried and heat treated at 300 ^{o}C in air in order to remove impurities. Iodine doping was carried out following the procedure published by Zhao et al.[11] DWNT fibers were placed in the iodine vapor at 473 K for 3 hrs. The DWNT fibers were placed in a stainless steel container with 0.5 g of iodine powder. Prior to heating, the container was evacuated to approximately 5kPa: Iodine vaporizes at 0.14MPa at the temperature 473K. For the heat treatment of DWNT-H_2O_2 in air, the fiber was placed in the furnace at room temperature, heated to the desired temperature and withdrawn from the furnace after 15 minutes.

The SWNTs used in this study are purified showing metallic (98%) and semiconductor (98%) content as purchased from Nano Integris in the form of buckypaper, the percentages reflect the metallic to semiconductor ratio or vice versa. The highly oriented pyrolytic graphite (HOPG) from SPI (Grade 1), and the graphite film is from the Panasonic Corporation. Multiwalled carbon nanotubes were synthesized by CVD with a mixture toluene/ethanol/ferrocene, and are labeled as MWNT-COx.[27] MWNTs doped with nitrogen were synthesized by CVD with a mixture of benzylamine/ferrocene, and labeled as MWNT-CNx.b28 The polyacrylonitrile (PAN) fibers T-300, were fabricated by Toray Industries, Inc. These carbon materials were held only to the H_2O_2 treatment, as described before.

The DWNT and DWNT-H2O2 samples were characterized by scanning electron microscopy (SEM) (HR-SEM, JSM-7000F/1V, JEOL), Raman spectroscopy (Renishaw in Via Raman microscope, 532 nm and 785 nm and T64000, Horiba Jobin Yvon 488 nm, 633 nm, 1064 nm). The fibers were dispersed ultrasonically in isopropanol in order to carry out transmission electron microscopy (TEM) studies (Cs-corrector (2) equipped with HR-TEM, JEM2100, JEOL, Japan). Surface chemical analysis was performed by X-ray photoelectron spectroscopy (XPS) using an Axis-Ultra, Kratos, UK apparatus. X-ray diffraction data was measured using a synchrotron radiation source at beam line BL04B2 of SPring-8 in Japan, where the x-ray wavelength is 0.0328 nm. Tensile tests were carried out with a Micro Strain Tester (Micro Autograph MST-I, Shimadzu). Resistivity and magnetoresistance measurements of the different fiber samples were carried out using a Quantum Design physical properties measurement system (PPMS), where a four-probe configuration was used by attaching the electrodes with silver paint with an inner electrode distance of approximately 1.5 mm. The applied current was fixed at 100 µA and the voltage was monitored. Prior to the measurements, the fibers were heated up to 100 ^{o}C for one hour within the equipment. The resistivity measurements

ARTICLE

were carried out between 380 K and 2K, and the magnetoresistance measurements were made between -6 and 6 T at 2 K.

Results & discussion

Scanning electron microscopy (SEM) images depict DWNT fibers before and after the H_2O_2 treatment (see Figure 1). The pristine DWNT fiber was soaked in acetone and twisted, giving an average fiber diameter of ca. 217 μm (Figure 1a,c and d). The resulting DWNT fiber was then sonicated in H_2O_2 and dried in air, and during the H_2O_2 treatment the fiber exhibits a volume expansion due to a partial de-bundling of the DWNTs (diameter ca. 500 μm, Figure 1b), due to the H_2O_2 wetting; a volume expansion is also observed when soaking DWNTs in sulfuric acid.[11] When drying, the fibers became "flat" on the drying substrate due to the removal of the solvent and to the surface tension during evaporation. Therefore, the fiber was soaked in acetone again and twisted after the H_2O_2 treatment, in order to obtain a fiber that could be handled for further characterization (average fiber diameter of ca. 95 μm, Figure 1f and g). The densities of the fibers, before and after the H_2O_2 treatment with further twisting, increased from 0.21 g/cm^3 to 1.29 g/cm^3. This densification could partially aid in the decrease in electrical resistivity, providing an increase in ohmic contact among DWNTs throughout the entire fiber. From the SEM studies, a reduction of the metal nanoparticle content within the fibers was observed for the DWNT-H_2O_2 in Figure 1h relative to Figure 1e. Transmission electron microscope (TEM) images reveal that pristine DWNTs initially contained some amorphous carbon as well as iron nanoparticles encapsulated within carbon shells (see Figure SI1). After the H_2O_2 treatment some of the DWNTs break and many of these iron nanoparticles were removed, leaving behind hollow carbon shells and amorphous carbon (see Figure SI1e and f).[11,12] The

area of the carbon materials and iron was measured from the TEM images and the iron content area was calculated. DWNT and DWNT-H_2O_2 fibers exhibit a content of 1.28% and 0.71% iron based on the area of the iron nanoparticles from the TEM images, respectively (see Figure 1e and h). Hydrogen peroxide cracks the amorphous carbon enabling the catalyst particles to be exposed and to react with H_2O_2 following the Fenton reaction.[29,30] The encapsulation of the iron particles could decrease their reactivity, therefore leaving amorphous carbon and carbon shell material within the fiber. In addition, some DWNTs partially break as a result of these treatments.

We recorded Raman spectra using different laser excitation energies (2.33 eV and 1.96 eV) on DWNT fibers before and after H2O2 treatment in order to monitor structural changes, and to observe different behaviors in the radial breathing modes. In Figure 2a, the radial breathing mode (RBM) is depicted. Here two regions can be observed: the inner walls above 190 cm^{-1} (1.2 nm) and the outer walls below 190 cm^{-1}.[31-33] There are four possible configurations for semiconducting and metallic tubes within DWNTs (i.e., S@M, S@S, M@M and M@S). It is important to emphasize that an inner S tube that is in resonance with a certain E_{laser} will possess S or M outer tubes that in general are not in resonance with the same E_{laser} as the inner tube, and the same situation applies to inner M tubes.[32] The diameters were calculated according to the equation $\omega_{RBM} = 218.3/d_t + 15.9$, where ω_{RBM} is in cm^{-1}.[32-34] The assignment of the outer and inner nanotubes was carried out by TEM observations, where the full width half maximum (FWHM) linewidths for the outer tubes were between 1.16 nm and 1.83 nm and for the inner tubes were between 0.52 nm to 1.32 nm (see Figure SI2). Figure 2a highlights the transition energies at different laser energies according to the theoretical
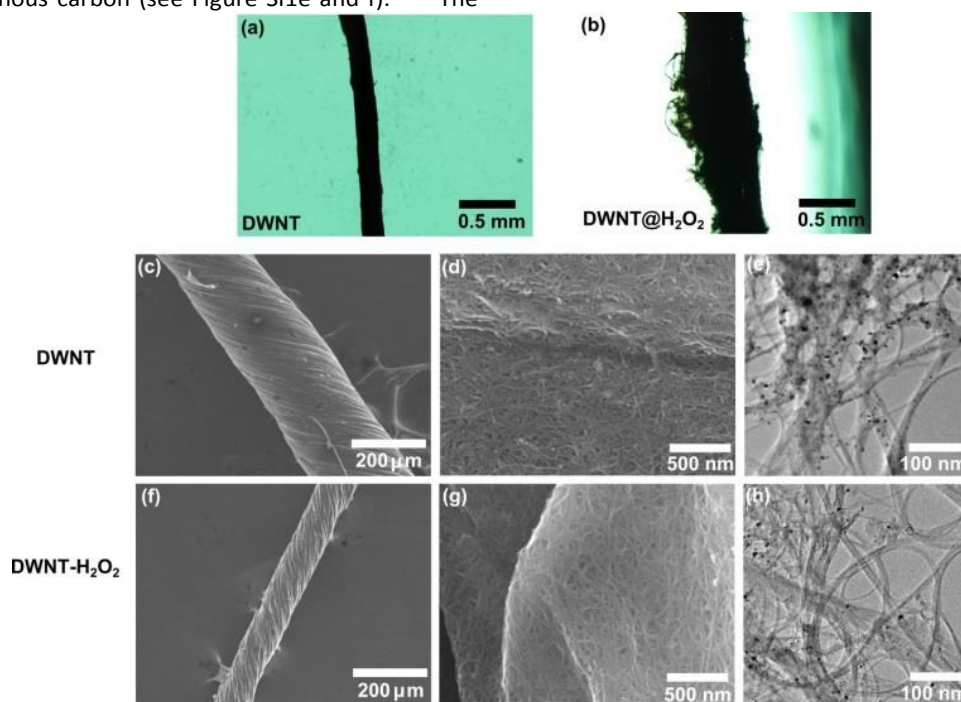
Figure 1: Optical microscope images of the fibers (a) a pristine (DWNT) and (b) the DWNT just after H_2O_2 treatment. (c,d,f,g) scanning electron microscope image, transmission electron microscope images of (e) pristine (DWNT) and (h) the DWNT after H_2O_2 treated and further twisting (DWNT-H_2O_2). Here the fiber has an increase in volume after H_2O_2 treatment and its diameter is reduced further by twisting. TEM images exhibit iron nanoparticles within the fiber.

Journal Name

ARTICLE

Kataura plot.[35,36] The semiconducting nanotubes with diameters between 0.86 nm and 1 nm have Raman peak intensities in the range 220 cm^{-1} – 270 cm^{-1} and are closer to their resonant energies when irradiated with the 1.69 eV laser, while the peak intensities for the outer tubes were observed mainly with 2.33 eV laser irradiation both for the pristine DWNTs and for the H_2O_2 treated DWNTs. With both laser energies it is evident that their intensities are greatly decreased when treated with H_2O_2. The variation in intensity could arise from the oxidation using H_2O_2 and from a decrease in the content of small diameter CNTs.[27,28,37,38] Doping effects from residual H_2O_2 or other by-products from the chemical treatment are not considered because the Raman measurements were made after drying the samples.

The D-band region suggests disorder and symmetry-breaking within carbon materials. It is well known that H_2O_2 can act as a soft oxidizer for carbon materials. Therefore, after several hours of H_2O_2 treatment some structural disorder could arise within the sample due to breakage of the C-C bonds into oxygenated functionalities.[39] The intensity ratio between the D-band and the G-band (I_D/I_G) is shown in Table 1 and Figure SI3a. In this particular case, the H_2O_2 treatment did not significantly affect the I_D/I_G ratio. This is in agreement with the results of Miyata et $al.$ who also did not observe any change in the I_D/I_G ratio.[18] However, these authors used a purified nanotube sample before the H_2O_2 treatment,[24] which differs from the procedure reported here. In the G-band region from 1500 to 1650 cm^{-1} we can see two peaks in the Raman spectra of Figure 2b, labeled here as the G+ and G- peaks centered at cm-1 > 1590 cm-1 and < 1590 cm^{-1}, respectively (see Figure 2b). The G+ peak is associated with carbon atoms vibrations along the axis of the carbon nanotube, whereas the G- intensity corresponds to carbon atoms on the outer, larger diameter tube of the DWNT.[40] The G- shape is sensitive to semiconducting tubes with Lorentzian line shapes as well as to metallic tubes with Breit–Wigner–Fano line shapes.[40] The G-region is also dependent upon d_t, in which the smaller diameter CNTs exhibit a lower Raman frequency shift.[41] The shape of the G band depends upon which CNT layer is in resonance at a given value of E_{laser}.[42] For the DWNT-H_2O_2 tubes, the intensity of the G- shoulder (above 1550 cm-1) is slightly increased when excited by the laser of 1.69 eV. However, the G- shoulder below 1546 cm^{-1} exhibits a lower intensity at the 2.33 eV laser energy excitation, in agreement with the overall decrease of the intensity observed for the inner nanotubes, with regard to their RBM vibrations measured in this study. Changes in the intensity of the G-region could be due to charge-transfer in the Lorentzian and the Breit–Wigner–Fano line shapes,[43] and the changes may come from oxidation effects, which are observed by comparing spectra for the pristine and H_2O_2 treated tubes.

SWNTs exhibit two G'-band peaks for an individual SWNT, and these arise from double resonance processes. In addition, the position of these peaks can depend on the tube diameter; small diameter tubes exhibit a lower Raman G' frequency shift and larger diameter tubes present a higher Raman frequency shift in the G'-band spectra.[40,42,43] Therefore, for DWNTs one can expect four peaks, two of them corresponding to the inner nanotubes and the other two for the outer tubes.[32] At higher E_{laser} the G' peaks are more separated and it becomes easier to analyze the G' spectra from DWNTs. For this reason we used E_{laser} = 2.33 eV to analyze the details of the G' lineshape.[32] From the G' peak of DWNT-H_2O_2 (see Figure 2c), the two deconvoluted peaks at lowest frequency exhibit a lower intensity than those for the pristine DWNT. This suggests that a decreased contribution comes from the signal of small diameter nanotube walls, and this interpretation is in accordance with the observations from the RBM and G-band from this sample.

Table 1 Analysis of Raman spectra at the 532 nm (2.33 eV) laser line.

	I_D/I_G	G'1 (cm^{-1})	G'2 (cm^{-1})	G'3 (cm^{-1})	G'4 (cm^{-1})
DWNT	0.037	2627	2648	2665	2692
DWNT-H_2O_2	0.038	2638	2662	2676	2701

I_D/I_G is the ratio of the D-band and G-band peak intensity. The G'-band was deconvoluted into four peaks where G'1, G'2, G'3, and G'4. Furthermore, G'1 and G'2 correspond to the inner walls and G'3 and G'4 correspond to the outer walls of the DWNTs.

In order to confirm the observations obtained by Raman spectroscopy for semiconducting nanotubes, the same methodology was applied to pure metallic (M-SWNT) and to pure semiconducting (S-SWNT) single-walled carbon nanotubes (see Figures SI4 and SI5). From these observations, it was found that semiconducting nanotubes exhibit a greater change in the RBM line shape when compared with metallic SWNTs. Small angle X-Ray diffraction (XRD) was performed on the pristine and H_2O_2 treated DWNT fiber (see Figure SI6). The XRD results that were thus obtained exhibited two peaks: one broad peak at 4.9 o 2θ was assigned to the (002) graphitic plane of the DWNT and for the amorphous carbon, and another peak at 9.2 o 2θ which can be assigned to the (110) plane of the iron catalyst. After the H_2O_2 treatment the 9.2 o 2θ peak intensity is decreased, suggesting the removal of the iron catalyst via the Fenton reaction with H_2O_2.[29,30]

Journal Name

ARTICLE
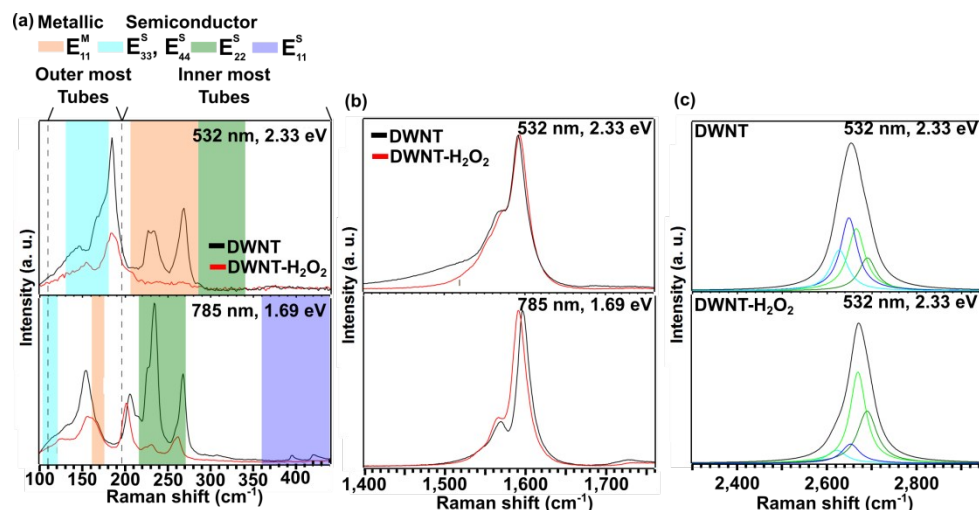
Figure 2: Raman spectroscopy measurements of the (a) radial breathing modes (RBM), (b) G-band and (c) G'-band of the pristine (DWNT, black line) and H_2O_2 treated (DWNT-H_2O_2, red line) double walled carbon nanotube fiber. The measurements in (a), (b), (c) were performed with 2.33 eV laser energy and spectra are also shown for RBM and G band for 1.69 eV laser energy. All the spectra were normalized relative to the G-band.

X-ray photoelectron spectroscopy (XPS) was carried out in order to elucidate the surface chemical composition of the fiber before and after the H_2O_2 treatment. In the C1s peak, components with binding energy corresponding to sp^2 hybridization was observed at 284.3 eV and a smaller contribution corresponding to sp^3 hybridized carbon were observed within the same peak (see Figure 3a).[44,45] At 285.8 eV, the peak was assigned to C-O and a new peak located at 286.8 eV with low intensity arises after the H_2O_2 treatment, which corresponds to C=O functionalization (see Figure 3c).[29,46] This type of functionalization has been reported for H_2O_2 treatment on MWNTs, and may also be attributed to the oxidation of amorphous carbon due to its higher chemical reactivity.[24,47] From the semi-quantitative elemental analysis, the oxygen content increases from 3.96 at. % to 13.63 at. % (see Figure 3b,d and Table SI1), due to the mild oxidation of the fibers. In addition, a smaller amount of iron was still present after the H_2O_2 treatment.

The electrical transport measurements of the fibers were carried out using a physical property measurement system (PPMS). Interestingly, the room temperature resistivity of the pristine DWNT fibers was found to be ca. 4.19×10^{-3} $\Omega \cdot cm$ and for DWNT-H_2O_2 the value decreased to 2.77×10^{-4} $\Omega \cdot cm$, more than an order of magnitude lower than that of the pristine fiber. The H_2O_2 treatment was repeated on five different DWNT fibers from different synthesis batches and the average obtained resistivity value after treatment is 4.44×10^{-4} $\Omega \cdot cm$ and values vary $\pm 3 \times 10^{-4}$ $\Omega \cdot cm$. The resistivity value obtained here is lower than that reported by Wei et al. who have also

treated DWNTs with H_2O_2; however, Wei et al. used a film morphology[12] in comparison to our nanotube fiber
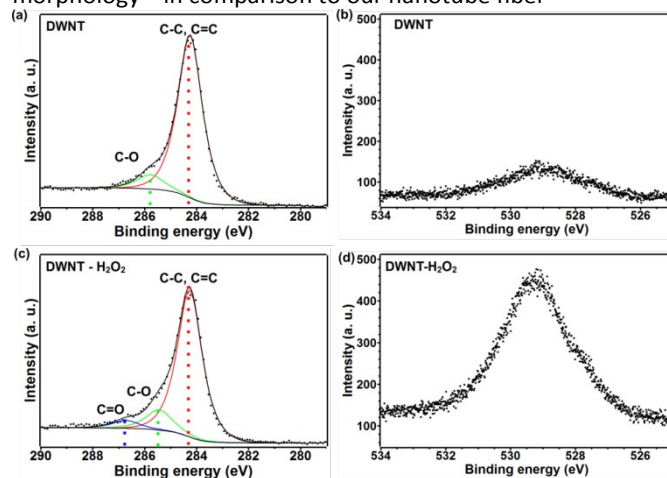
Figure 3: X-Ray photoelectron spectroscopy: (a,c) for the C 1s XPS signal and (b,d) for the O 1s XPS signal of the (top) pristine DWNT and (bottom) H_2O_2 treated (DWNT-H_2O_2) fibers. After the H_2O_2 treatment there is a clear introduction of C-O functionalities and a more intense XPS O 1s peak is seen within the sample. The intensity scales in (a) and (c) are different, however, the intensity scales are the same for (b) and (d), to demonstrate the higher oxygen presence more qualitatively within the DWNT-H_2O_2 fibers.

morphology. This difference in sample electrical resistivity could be caused by the promotion of a better wetting during our H_2O_2 treatment, which is consistent with our much larger expansion of the fiber during the H_2O_2 treatment.

Furthermore, our DWNTs-H_2O_2 behave like a metal at temperatures above 100 K due to the decrease in electrical resistivity with decreasing temperature, and at lower temperatures the sample behaves like a semiconductor with increasing resistivity while lowering the temperature (see Figure 4a and b). However, untreated DWNTs behave like a semiconductor over the entire temperature region. Our data (Figure 4 and SI7) were fitted according to the variable range hopping (VRH) model $\rho(T) = \rho_0 \exp[-T_0/T]^{1/(d+1)}$ for d = 1, 2 and 3.[48] Interestingly, before the H_2O_2 treatment, the DWNTs fit better for d=1 and after the H_2O_2 treatment the fit is better for d = 3. These results were obtained by fitting the best R^2 value for the linear regression fittings applied to each d value (see Figure SI7 and Table SI2). The normalized resistivity value at 2 K ($\rho(2K)/\rho(300K)$) decreased from 24.23 to 1.16 for DWNT-H_2O_2. The transverse magnetoresistance (MR%) measurements (see Figure 4c) revealed that in the low magnetic field regime (< 1.5 T), all samples exhibited negative MR%, with a $H^{1/2}$ dependency, which is an indication of weak localization, as has been observed for SWNTs.[49,50] At higher magnetic fields (> 1.5 T) the DWNT sample followed a positive MR% as H^2, which could be attributed to a spin-dependent variable range hopping conduction mechanism (see Figure 4c). The DWNT-H_2O_2 sample preserves a negative MR% throughout the measured magnetic fields (-6 T to 6 T) (see Figure 4c), and a similar behavior has been observed for strongly p-doped SWNTs.[16] In order to compare the effects of H_2O_2 with other intercalates, DWNT fibers were also treated with: thionyl chloride (DWNT-$SOCl_2$), silver nanoparticles (DWNT-Ag NP), ammonium hydroxide (DWNT-NH_3) and iodine (DWNT-I) (see Figure 4a and b). For DWNT-$SOCl_2$ and DWNT-NH_3, shorter times were used due to the complete decomposition of the fiber morphology after prolonged sonication. We noted that all of these agents could significantly decrease the resistivity, except for DWNT-NH_3 which has been chosen in pursuit of possible n-type doping. For example, DWNTs-$SOCl_2$ and DWNTs-I exhibit low electrical resistivity values in the order of 10^{-4} Ω·cm, in which DWNT-$SOCl_2$ exhibits the lowest value of 3.29×10^{-4} Ω·cm, close to that of DWNT-H_2O_2 (see Table 2). The treatments with iodine, thionyl chloride and hydrogen peroxide showed an increase in fiber density after the final twisting step (see Table 2). This suggests that the intercalants and functionalization may well help to densify the fibers, thus decreasing the electrical resistivity. All the agents used (except for ammonium hydroxide) caused the DWNT fibers to behave as metals at temperatures above 200 K (see Figure 4b). It might be possible that the metallic-like nanotubes dominate the electrical transport at high temperatures due to the increase in ohmic contact among the CNTs by an increase in fiber density and the removal of small diameter CNTs which could exhibit a larger band gap.[35,51] At lower temperatures the structural defects (i.e. vacancies and oxidation-related groups) and intertube coupling give rise to charge localization effects that give the nanotubes a semiconductor behavior.[52] We omitted the effect of H_2O_2 doping, because of the drying step after H_2O_2 treatment and the need of heating the fibers at 100 ^{o}C within the PPMS, when we measured the electric transport.

All the p-type doping agents exhibit a negative MR, and the DWNT-NH_3 sample displays a positive MR, at 2 K (see Figure 4c and Table 2). These comparisons confirm that high electrical conductivities could be achieved with an environmentally friendly chemical such, as H_2O_2.

Table 2 Electrical properties and density of the modified double walled carbon nanotubes.

Sample	Resistivity*	MR**	Density	Specific conductivity
	Ω cm		mg mm^{-3}	S m^2 kg^{-1}
DWNT	4.19×10^{-3}	Positive	0.21	113.33
DWNT -$SOCl_2$	3.29×10^{-4}	Negative	1.15	263.88
DWNT -Ag NP	3.52×10^{-3}	Negative	0.10	268.41
DWNT -NH_3	4.78×10^{-3}	Positive	0.58	35.98
DWNT -I	6.10×10^{-4}	Negative	1.05	186.61
DWNT -H_2O	6.29×10^{-3}	Positive	0.56	28.11
DWNT -H_2O_2	2.77×10^{-4}	Negative	1.29	278.70

Results are given for pristine (DWNTs), DWNTs with silver nanoparticles (DWNT-Ag NP), DWNT soaked with NH_3 (DWNT-NH_3) and with $SOCl_2$ (DWNT- $SOCl_2$), DWNTs intercalated with iodine (DWNT-I) and H_2O_2 treated (DWNT-H_2O_2).
* Resistivity at 300 K
** MR magnetoresistance at 2 K

The samples were kept at room conditions for two months and the measured resistivity values exhibited a small resistivity increase to 4.307×10^{-4} Ω·cm from 2.77×10^{-4} Ω·cm. To rule out the effect of water adsorption, another fresh DWNT sample was sonicated in pure H_2O; a resistivity of ca. 6.29×10^{-3} Ω·cm was measured. The twisting effect was tested on a pristine DWNT fiber soaked in acetone. The fiber was fixed at both ends to a pair of clamps, and the resistivity was monitored after several turns or twists (see Figure SI8). The initial density of the fiber was 0.26 g/cm^3, and the density changed to 0.53 g/cm^3 after 60 turns (2.04 times higher), exhibiting a decrease in resistivity from 3.9×10^{-3} Ω·cm to 2.4×10^{-3} Ω·cm (1.62 times lower). Following the H_2O_2 treatments, the DWNT density changed from 0.21 g/cm^3 to 1.29 g/cm^3 (6.14 times higher), and the electrical resistivity changed from 4.19×10^{-3} Ω·cm to 2.77×10^{-4} Ω·cm (15.12 times lower). These results confirm that the fiber densification is also responsible for decreasing the electrical resistivity, along with the removal of small diameter CNTs that are predominantly semiconductors.

Journal Name
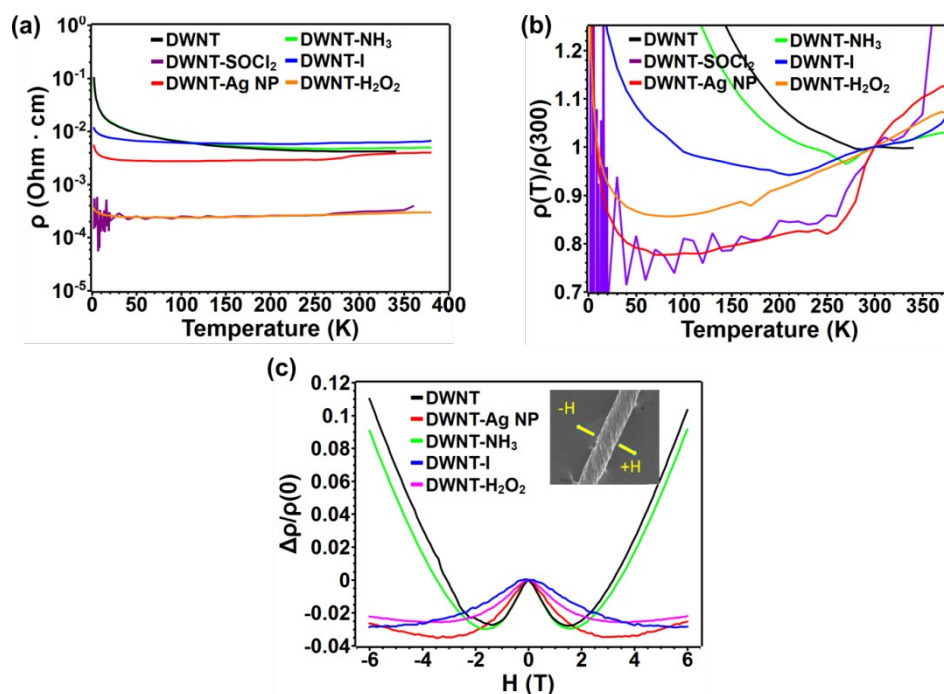
ARTICLE

Figure 4: (a) Resistivity and (b) normalized resistivity vs. temperature, and (c) magnetoresistance vs. magnetic field plots for the pristine (DWNTs), DWNTs with silver nanoparticles (DWNT-Ag NP), DWNTs soaked with NH_3 (DWNT-NH_3) and $SOCl_2$ (DWNT-$SOCl_2$), DWNT intercalated with iodine (DWNT-I) and H_2O_2 treated (DWNT-H_2O_2). The resistivity measurements were performed on the fibers in the temperature range between 2 K and 340 K and the magnetoresistance (MR) was measured at 2 K. The inset in (c) indicates the direction of the applied magnetic field perpendicular to the fiber axis. The MR for DWNT-$SOCl_2$ is not shown due to low signal to noise ratio.

The following mechanism is proposed in order to explain the decrease in the electrical resistivity of DWNT fibers. The analysis of the G-band and the G'-band data indicated the removal of small diameter carbon nanotubes, by a decrease in the intensity of the first two deconvoluted peaks in the G'-band observed when using a 532 nm excitation laser (Figure 2c). The higher oxidation reactivity towards smaller diameter carbon nanotubes has been observed by Zhou et al. for SWNTs, and a tendency was found for the presented H2O2 treatment.[53] There is a very low possibility that oxidation could have removed small diameter CNTs during laser irradiation from the Raman measurement,[25,37] because the inner wall tubes are protected by the outer wall tubes and residual H_2O_2 could have been removed during the drying process. XPS analysis revealed an increase in the oxygen content, which could be in the form of hydroxyl functional groups attached to the outer tubes. Whilst the hydrogen peroxide may decompose amorphous carbon and may later react with the iron nanoparticles following the Fenton reaction,[29] thus lowering the iron content almost by half when compared with the pristine sample.

In addition, the degree of purification is less than that reported by Wei et al. (see Figure 1e,h and Figure SI1), who have observed a decrease in electrical resistivity by one order of magnitude after DWNT purification.[12] Therefore, our purification method may only affect in a small way the degree of decrease of the electrical resistivity. In this context, we noted that after sonicating the DWNT fibers in the presence of pure H_2O there is no decrease in electrical resistivity (see Table 2). The twisting experiments demonstrate that increasing the fiber density could slightly decrease the electrical resistivity by allowing better electrical contact points among the DWNTs with each other (see Figure SI8). A complementary experiment consisting of the sonication in pure H_2O indicated that the H_2O_2 treatment could have an etching effect with narrow diameter tubes that are more reactive. Because DWNT synthesis tends to yield more semiconducting than metallic CNTs, the removed small diameter nanotubes are mostly semiconducting, as observed by Raman spectroscopy (see Figure 2); a more metallic sample was observed by the resistivity vs. temperature measurements (see Figure 4), which is in agreement with the observations from Lekawa-Raus et al. who found similar trends in resistance-temperature dependence for CNT fibers with high metallic SWNT content.[54]

The mechanical properties of DWNT fibers were also measured, and the Young moduli of 4.14 MPa and 1.44 MPa were recorded for the pristine and H_2O_2 treated fibers, respectively. The tensile strength decrease from 50 MPa to 15 MPa, is possibly due to the formation of partial DWNT ruptures caused by the H_2O_2 treatment. Despite these relatively low tensile strength values, it was possible to handle and manipulate DWNT fibers, with the possibility of even making knots and twists with them (see Figure 5a and b). Therefore, we believe that it is possible to use these fibers as electrical conducting cables.

In order to illustrate this application, a working lighting device was assembled with a battery and a light emitting diode (LED) (see Figure 5c). In order to demonstrate the versatility of the H_2O_2 treatment, we also sonicated other forms of carbon in H_2O_2, such as highly oriented pyrolytic graphite (HOPG), a graphite film, a DWNT fiber, MWNTs made by toluene/ethanol/ferrocene (MWNT-COx),[27] nitrogen doped MWNTs (MWNT-CNx)[28] and carbon fibers (PAN-fiber) (see Figure 5d). The materials that already exhibit resistivity values of ca. 10^{-4} or lower (HOPG and the graphite film, without twisting) did not show any further decrease in resistivity after H_2O_2 treatment. MWNT-COx film (without twisting) initially exhibited an electrical resistivity of 6.61×10^{-2} $\Omega \cdot cm$ and the value is increased to 1.58×10^{-1} $\Omega \cdot cm$ after the H_2O_2 treatment, perhaps due to a severe oxidation during the treatment.[39] For MWNT-CNx film (without twisting), the resistivity decreased from 0.514 $\Omega \cdot cm$ to 0.107 $\Omega \cdot cm$, and in this scenario it is possible that the nitrogen sites may catalyze the decomposition of H_2O_2. This special case involves different interactions and will be published elsewhere. Carbonized PAN-fibers exhibited an increase of electrical resistivity from 3.41×10^{-3} $\Omega \cdot cm$ to 6.09×10^{-3} $\Omega \cdot cm$, possibly due to the oxidation occurring at defect sites present within the material. DWNTs in the form of a fiber exhibit the largest change in resistivity (from 4.19×10^{-3} $\Omega \cdot cm$ to 3.77×10^{-4} $\Omega \cdot cm$), which may be due to the particular morphology that favors exohedral doping, and its special chemistry and degree of crystallinity within the DWNT fibers. Wei et al. studied DWNTs in the form of films which could have inhibited a good H_2O_2 wetting within the bulk sample[12] in the current case, the fiber de-bundling during the sonication suggested wetting with H_2O_2. In addition, the densification of the fiber after H_2O_2 treatment could result in a higher electrical percolation.

DWNT fiber. (d). The resistivity of different carbons after several hours of H_2O_2 sonication. The plots exhibit the variation in resistivity of the H_2O_2 treated carbon samples compared with the pristine counterparts for highly oriented pyrolytic graphite (HOPG), graphite film, DWNT-fiber, multiwalled carbon nanotubes made by toluene/ethanol/ferrocene (COx), nitrogen doped multiwalled carbon nanotubes (CNx) and carbon fiber (PAN-fiber).

Conclusions

In summary, the H_2O_2 treatment significantly decreased the electrical resistivity of DWNT fibers. A careful analysis of the Raman spectra, XPS and electrical transport data demonstrated that the H_2O_2 treatment results in the preferential removal of small diameter semiconducting CNTs. These processes are favored in the bundle structure and are observed by an increase in volume within the solution. Furthermore, an increase in fiber density could further increase the electrical contact among the DWNTs. The method used in this work could yield low resistivity metallic-like DWNT fibers with low cost and a facile implementation method, with similar results to those obtained using other hazardous chemical agents. The use of H_2O_2 treated DWNT fibers can be helpful in promoting the use of CNTs in industry where highly conducting and lightweight materials are required (e.g. power transmission lines). In addition, these low resistivity CNTs could be used in conjunction with ceramics, polymers, electronic devices, medicine, among many others.

Acknowledgements

Figure 5: Scanning electron microscope images of (a) a knot and (b) a highly twisted fiber. (c) Photograph of a device composed of a battery, a light emitting diode (LED) and the

Notes and references

1   A. Oberlin, M. Endo, T. Koyama. *J. Cryst Growth*. 1976, **32**, 335

2   M. Endo. *Chem. Tech.* 1988, **18**, 568

3   S. Iijima. *Nature* 1991,**354**, 56

4   S. Iijima, T. Ichihashi. *Nature* 1993, **363**, 603

5   E. T. W. Ebbesen, H. J. Lezec, H. Hiura, W. Bennett, H. F. Ghaemi, T. Thio. *Nature* 1996, **382**, 54

6   H. Dai, E. W. Wong, C. M. Lieber. *Science* 1996, **272**, 523

7   E. W. Wong, P. E. Sheehan, C. M. Lieber. *Science* 1997, **277**, 1971

8   A. Thess, R. Lee, P. Nikolaev, H. Dai, P. Pierre, J. Robert, C. Xu, Y. H. Lee, S. G. Kim, A. G. Rinzler, D. T. Colbert, G. E. Scuseria, D. Tománek, J. E. Fischer, R. E. Smalley. *Science* 1996, **273**, 483

9   J. E. Fischer, H. Dai, A. Thess, R. Lee, N. M. Hanjani, D. L. Dehaas, R. E. Smalley. *Phys. Rev. B* 1997, **55**, 4921

10   H. W. Zhu, C. L. Xu, D. H. Wu, B. Q. Wei, R. Vajtai, P. M. Ajayan. *Science* 2002, **296**, 884

11   Y. Zhao, J. Wei, R. Vajtai, P. M. Ajayan, E. V. Barrera. *Sci. Rep.* 2011, **1**, 83

12   J. Wei, H. Zhu, B. Jiang, L. Ci, D. Wu. *Carbon* 2003, **41**, 2495

13   G. Chen, D. N. Futaba, S. Sakurai, M. Yumura, K. Hata. *Carbon* 2014, **67**, 318

14   T. Enoki, M. Suzuki, M. Endo. Oxford University Press: Oxford, UK, 2003

15   B. Ruzicka, L. Degiorgi, R. Gaal, L. Thien-Nga, R. Bacsa, J.-P.Salvetat, L. Forro. *Phys. Rev. B* 2000, **61**, 2468

16   R. S. Lee, H. J. Kim, J. E. Fischer, A. Thess, R. E. Smalley. *Nature* 1997, **388**, 255

17   H. Tantang, J. Y. Ong, C. L. Loh, X. Dong, P. Chen, Y. Chen, X. Hu, L. P. Tan, L.-J. Li. *Carbon* 2009, **47**, 1867

18   Y. Miyata, K. Yanagi, Y. Maniwa, H. Kataura. *J. Phys. Chem. C* 2008, **112**, 3591

19   V. Skákalová, A. B. Kaiser, U. Dettlaff-Weglikowska, K. Hrnčariková, S. Roth. *J. Phys. Chem. B* 2005, **109**, 7174

20   U. Dettlaff-Weglikowska, V. Skákalová, R. Graupner, S. H. Jhang, B. H. Kim, H. J. Lee, L. Ley, Y. W. Park, S. Berber, D. Tománek, S. Roth. *J. Am. Chem. Soc.* 2005, **127**, 5125

21   N. Behabtu, C. C. Young, D. E. Tsentalovich, O. Kleinerman, X. Wang, A. W. Ma, E. A. Bengio, R. T. Waarbeek, J. J. Jong, R. E. Hoogerwerf, S. B. Fairchild, J. B. Ferguson, B. Maruyama, J. Kono, Y. Talmon, Y. Cohen, M. J. Otto, M. Pasquali. *Science* 2013, **339**, 182

22   R. Graupner, J. Abraham, A. Vencelová, T. Seyller, F. Hennrich, M. M. Kappes, A. Hirsch, L. Ley. *Phys. Chem. Chem. Phys.* 2003, **5**, 5472

23   J. D. Wiggins-Camacho, K. J. Stevenson. *J. Phys. Chem. C* 2009, **113**, 19082

24   Y. Miyata, Y. Maniwa, H. Kataura. *J. Phys. Chem. B* 2006, **110**, 25

25   M. Yudasaka, M. Zhang, S. Iijima. *Chem. Phys. Lett.* 2003, **374**, 132

26   S. Coskun, B. Aksoy, H. E. Unalan. *Cryst. Growth Des.* 2011, **11**, 4963

27   A. Botello-Méndez, J. Campos-Delgado, A. Morelos-Gómez, J. M. Romo-Herrera, A. G. Rodríguez, H. Navarro, M. A. Vidal, H. Terrones, M. Terrones. Chem. *Phys. Lett.* 2008, **453**, 55

28   M. Terrones, R. Kamalakaran, T. Seeger, M. Rühle, *Chem. Commun.* 2000, 2335

29   K. V. Voitko, R. L. D. Whitby, V. M. Gun'ko, O. M. Bakalinska, M. T. Kartel, K. Laszlo, A. B. Cundy, S. V. Mikhalovsky. *J. Colloid Interf. Sci.* 2011, **361**, 129

30   K. R. Moonoosawmy, P. Kruse. *J. Am. Chem. Soc.* 2010, **132**, 1572

31   J. Wei, B. Jiang, X. Zhang, H. Zhu, D. Wu. Chem. *Phys. Lett.* 2003, **376**, 753

32   F. Villalpando-Paez, H. Son, S. G. Chou, G. G. Samsonidze, Y. A. Kim, H. Muramatsu, T. Hayashi, M. Endo, M. Terrones, M. S. Dresselhaus. *Phys. Rev. B* 2009, **80**, 035419

33   A. Jorio, C. Fantini, M. A. Pimenta, R. B. Capaz, G. G. Samsonidze, G. Dresselhaus, M. S. Dresselhaus, J. Jiang, N. Kobayashi, A. Grüneis, R. Saito. *Phys. Rev. B* 2005, **71**, 075401

34   M. Endo, Y. A. Kim, T. Hayashi, H. Muramatsu, M. Terrones, R. Saito, F. Villalpando-Paez, S. G. Chou, M. S. Dresselhaus. *Small* 2006, **2**, 1031

35   H. Kataura, Y. Kumazawa, Y. Maniwa, I. Umezu, S. Suzuki, Y. Ohtsuka, Y. Achiba. Synthetic *Metals* 1999, **103**, 2555

36   G. G. Samsonidze, R. Saito, N. Kobayashi, A. Grüneis, J. Jiang, A. Jorio, S. Chou, G. Dresselhaus, M. S. Dresselhaus. *Appl. Phys. Lett.* 2004, **85**, 5703

37   J.-Y. Mevellec, C. Bergeret, J. Cousseau, J.-P. Buisson, C. P. Ewels, S. Lefrant. *J. Am. Chem. Soc.* 2011, **133**, 16938

38   S. Osswald, E. Flahaut, Y. Gogotsi. *Chem. Mater.* 2006, **18**, 1525

39   Y. Peng, H. Liu. *Ind. Eng. Chem. Res.* 2006, **45**, 6483

40   M. S. Dresselhaus, G. Dresselhaus, R. Saito, A. Jorio. *Phys. Rep.* 2005, **409**, 47

41   A. Jorio, A. G. Souza Filho, G. Dresselhaus, M. S. Dresselhaus, A. K. Swan, M. S. Ünlü, B. B. Goldberg, M. A. Pimenta, J. H. Hafner, C. M. Lieber, R. Saito. *Phys. Rev. B* 2002, **65**, 155412

42   F. Villalpando-Paez, H. Son, D. Nezich, Y. P. Hsieh, J. Kong, Y. A. Kim, D. Shimamoto, H. Muramatsu, T. Hayashi, M. Endo, M. Terrones, M. S. Dresselhaus. *Nano Lett.* 2008, **8**, 3879

43   A. G. Souza Filho, A. Jorio, G. G. Samsonidze, G. Dresselhaus, M. A. Pimenta, M. S. Dresselhaus, A. K. Swan, M. S. Ünlü, B. B. Goldberg, R. Saito. *Phys. Rev. B* 2003, **67**, 035427

44   W.-J. Chou, C.-C. Wang, C.-Y. Chen. J. *Inorg. Organomet Polym.* 2009, **19**, 234

45   H. Ago, T. Kugler, F. Cacialli, W. R. Salaneck, M. S. P. Shaffer, A. H. Windle, R. H. Friend. *J. Phys. Chem. B* 1999, **103**, 8116

46   S. Kundu, Y. Wang, W. Xia, M. Muhler. *J. Phys. Chem. C* 2008, **112**, 16869

47   J. T. Han, S. Y. Kim, J. S. Woo, H. J. Jeong, W. Oh, G.-W. Lee. *J. Phys. Chem. C* 2008, **112**, 15961

48   B. I. Shklovskii, A. L. Efros. Electonic Properties of Doped Semiconductors, In Springer Series in Solid-State Sciences; M. Cardona, P. Fulde, H.-J. Queisser, Eds.; Springer: Berlin, 1984

49   J. Vavro, J. M. Kikkawa, J. E. Fischer. *Phys. Rev. B* 2005, **71**, 155410.

50   G. T. E. Kim, S. Choi, D. C. Kim, D. S. Suh, Y. W. Park, K. Liu, G. Duesberg, S. Roth. *Phys. Rev. B* 1998, **58**, 16064

51   J. N. Wang, X. G. Luo, T. Wu, Y. Chen. *Nat. Comm.* 2014, **5**, 3848

52   J. M. Marulanda, Carbon Nanotubes, InTech Vukovar, 2010, 123

53   W. Zhou, Y. H. Oou, R. Russo, P. Papanek, D. E. Luzzi, J. E. Fischer, M. J. Bronikowski, P. A. Willis, R. E. Smalley. *Chem. Phys. Lett.* 2001, **350**, 6

54   A. Lekawa-Raus, K. Walczak, G. Kozlowski, M. Wozniak, S. C. Hopkins, K. K. Koziol. *Carbon* 2015, **84**, 118